Superconductivity and Cryogenics
Vol.11, No.4, (2009), pp.16~19

Growth behavior of YBCO films on STO substrates with ZnO nanorods

Se-Kweon Oh[1], Cho-Yeon Lee[1], Gun-Eik Jang[1,*], Kyoung-Won Kim[2], Ok-Bae Hyun[3]

[1]Department of Advanced Materials Engineering, Chungbuk National University, Cheongju 361-763, Korea
[2]Korea Institute of Science and Technology, Seoul 136-791, Korea
[3]Korea Electric Power Research Institute, DaeJeon 305-380, Korea

Received 9 November 2009; accepted 19 November 2009

Abstract-- **The influence of nanorods grown on substrate prior to YBCO deposition has been investigated. We studied the microstructures and characteristic of $YBa_2Cu_3O_{7-\delta}$ films fabricated on $SrTiO_3$ (100) substrates with ZnO nanorods as one of the possible pinning centers. The growth density of ZnO nanorods was modulated through Au nanoparticles synthesized on top of the STO(100) substrates with self assembled monolayer. The density of Au nanoparticles is approximately 240~260 μm^{-2} with diameters of 41~49 nm. ZnO nanorods were grown on Au nanoparticles by hot-walled PLD with Au nanoparticles. Typical size of ZnO nanorod was around 179 nm in diameter and 2~6 μm in length respectively. The ZnO nanorods have apparently randomly aligned and exhibit single-crystal nature along (0002) growth direction. Our preliminary results indicate that YBCO film deposited directly on STO substrate shows the c-axis orientation while YBCO films with ZnO nanorods exhibit any mixed phases without any typical crystal orientation.**

1. INTRODUCTION

Extensive studies are currently being carried out worldwide on $REBa_2Cu_3O_y$ (REBCO, RE = rare earth elements) coated conductors to be used in numerous potential applications such as superconducting fault current limiter (SFCL), cable, motors. To be suitable for power applications, REBCO coated conductors should have large critical current density (J_c) in high applied magnetic fields [1]. It is known that defects within high-temperature superconductors can pin the magnetic flux lines, so that large currents can flow through the materials in the presence of high applied magnetic fields. The flux pinning forces from naturally introduced pinning centers during the fabrication process. These defects such as oxygen vacancies, dislocations and twin boundaries are not enough to achieve high critical current density in high applied magnetic fields.

To increase the density of defects for effective pinning, there have been extensive studies on introducing artificial pinning centers. Nanoparticles and nanorods of non-superconducting materials are the candidates for strong artificial pinning centers in REBCO films. For the last few years, a significant improvement of J_c has been demonstrated in REBCO films with APCs such as Y_2BaCuO_5[2], Y_2O_3[3], $BaZrO_3$[4] and $BaSnO_3$[5]. Among these various APC proposals, $BaZrO_3$ nanorods have been successfully introduced into HTS films produced by pulsed laser deposition using $BaZrO_3$-doped YBCO targets. $BaZrO_3$ nanorods elongated along the c-axis were embedded in REBCO matrix, and these work as effective pinning centers[4].

On the other hand, we propose our strategy to induce the columnar defects by ZnO nanorods fabricated on the surface of substrate prior to the deposition of YBCO films. It has been reported that ZnO nanorods were grown on STO (100) substrates[6]. To be applicable for artificial pinning centers, the density of ZnO nanorods should be controlled. The growth density of ZnO nanorods is modulated through controlling of density of Au nanoparticles dispersed onto the substrate.

In this work, we investigated growth behavior and electric characteristic of YBCO films fabricated on the surface of STO substrates with ZnO nanorods. The YBCO films and nanorods were grown by using hot-walled pulsed laser deposition technique. The growth density of ZnO nanorods was modulated through Au nanoparticles synthesized on top of the substrates with self assembled monolayer and different deposition time.

2. EXPERIMENTAL

2.1. Gold nanoparticles synthesis

Gold nanoparticles were prepared by a chemical reduction method [7]. 80 ml distilled water and 1 mg $HAuCl_4$ was mixed together, and then it was heated up to 60 °C with vigorous magnetic stirring. An addition of 20 ml water solution with 0.05 mg trisodium citrate and 0.01 mg tannic acid was added. Afterwards, the aqueous solution was heated to boiling for an additional 15 min. After returning to room temperature, colloidal Au nanoparticles are formed in the solution.

2.2. Construction of gold nanoparticle arrays

The Au nanoparticle arrays were fabricated upon a STO

* Corresponding author: gejang@chungbuk.ac.kr

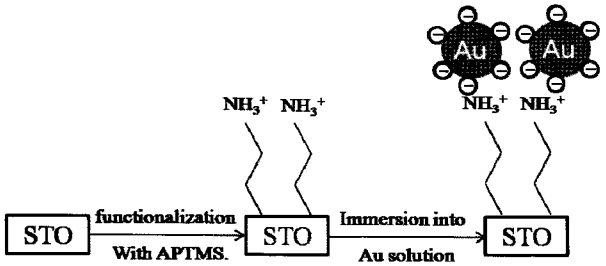

Fig. 1. Schematic representation for the chemical self assembly deposition process of Au nanoparticles.

(100) substrate. Prior to construction, the STO substrate was thoroughly cleaned in acetone, ethanol and deionized water for 15 min under ultrasonic agitation followed by drying with nitrogen gas. Then, it was pretreated in oxygen plasma for 20 min, modified by putting the STO substrate in a solution of aminopropyltrimethoxysilane (APTMS) in methanol at room temperature for 1h. The substrate was washed with methanol and deionized water and dried in oven at 70 °C for 20 min. The substrate was subsequently immersed in Au colloidal solution. The deposition time for Au nanoparticles were varied from 10 and 12 h, after which the STO substrate was extensively rinsed with deionized water. Figure 1 shows schematic representation for the cheminal self assembly deposition process of Au nanoparticles. Surface morphology of the Au nanoparticles on the substrates was investigated by atomic force microscopy (AFM) and scanning electron microscopy (SEM).

2.3. Fabrication of ZnO nanorods

ZnO nanorods were synthesized by hot-walled pulsed laser deposition (HW-PLD) using KrF excimer laser (248nm) with pulse repetition rate of 5~10 Hz. The nanorods were grown on STO substrates with assembled Au nanoparticles in an atmosphere of 1.2 Torr of flowing Ar at 800 °C. A distance between substrate and target was set at 25 mm and laser energy density on the target 1.2 J/cm^2. Deposition time was 5, 10 and 15 min. The synthesized ZnO nanorods were characterized using SEM, high-resolution transmission electron microscopy (HR-TEM) equipped with selected area electron diffraction (SAED) and photoluminescence (PL) spectroscopy.

2.4. Deposition of YBCO

YBCO films were deposited on STO substrates with ZnO nanorods by PLD at a substrate temperature of 820 °C under an oxygen partial pressure of 200 mTorr. A distance between substrate and target was set at 58 mm and a laser energy density on the target was 2 J/cm^2. After deposition, the YBCO films were annealed for 1 h at 500 °C at a pressure of 550 Torr of oxygen. The deposited YBCO films were characterized using SEM, X-ray diffraction (XRD) with the Cu-Kα radiation. The resistance was measured using the standard four-probe technique.

3. RESULTS AND DISCUSSION

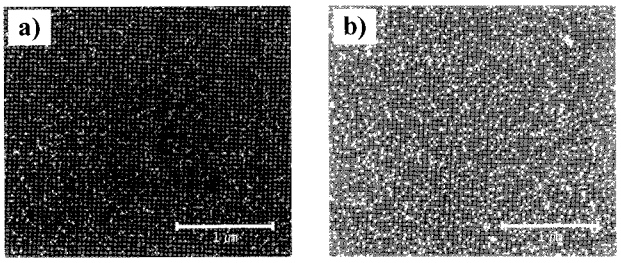

Fig. 2. SEM images of Au nanoparticles on the STO (100) surfaces with different deposition times in Au colloidal solution: (a) 10 hours and (b) 12 hours.

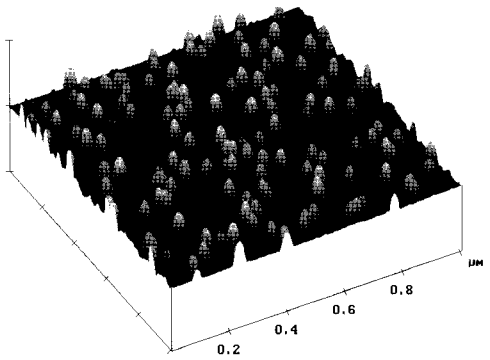

Fig. 3. The 3-Dimensional AFM image (1 x 1 μm) of Au nanoparticles on the STO after immersing for 12 hours in Au colloidal solution.

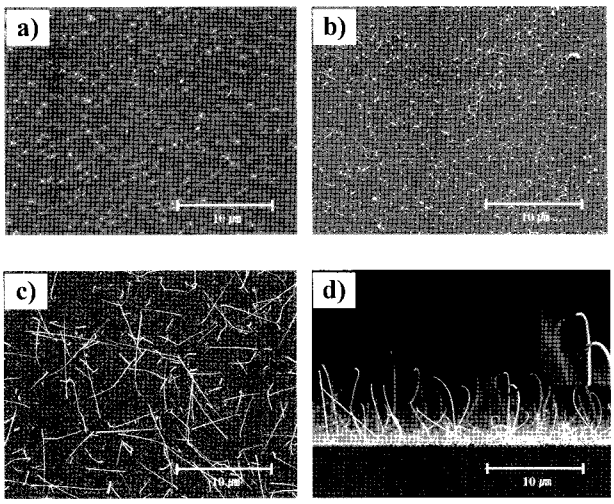

Fig. 4. SEM images of ZnO nanorods grown on Au nanoparticles / STO for different times: (a) 5min, (b) 10 min, (c) 15 min (surface) and (d) 15 min (cross-section).

The surface SEM images of Au nanoparticles coated on STO substrates modified with APTMS solution for 10 and 12 hours are shown Figure 2. As can be seen, the presence of many Au nanoparticles homogeneously distributed on the substrate surface is confirmed. As the time of deposition was 10 hours, the density of nanoparticles was 120 ~ 140 μm^{-2}. By increasing the time of deposition to 12

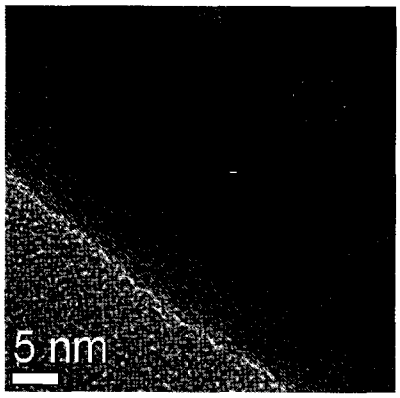

Fig. 5. High resolution TEM image of the ZnO nanorods on STO substrate. Inset: Selected area electron diffraction pattern.

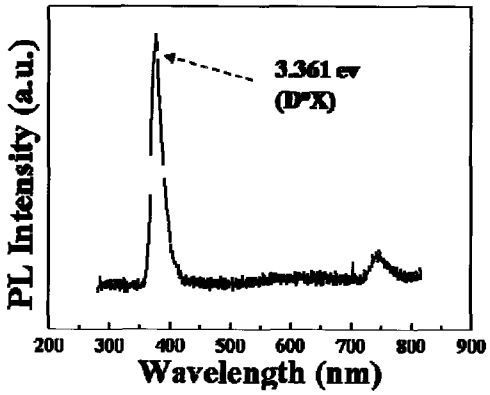

Fig. 6. PL emission spectrum of ZnO nanorods grown on STO substrate.

hours, the nanoparticle density increased up to 240 ~ 260 μm^{-2}. The particle density can be further increased with growth time. However, condensed particles were partially found in Figure 2 (b).

Figure 3 shows a AFM image of Au nanoparticles arrays fabricated on STO substrate chemically modified by the formation of a self-assembled monolayer under 12 hours growth time. The size of Au nanoparticles synthesized on STO substrates was around 29 ~ 32 nm in height and 41 ~ 49 nm in diameter.

The surface SEM images of aligned ZnO nanorods grown on a STO substrate as catalyzed by assembled Au nanoparticles (Figure 2b) for varying from 5, 10 and 15 min are shown in Figure 4. When ZnO nanorods were grown for 5 and 10 min, the size of nanorods were few and small. Typical size of ZnO nanorods grown for 15 min was around 179 nm in diameter and 2~6 μm in length respectively. SEM images also show that the nanorods have apparently randomly aligned and a thin film exists on the substrate surface. The inset in Figure 4d shows the bent ZnO nanorod.

Figure 5 shows high-resolution transmission electron microscopy (HR-TEM) image of the products of customized PLD. Clear image, indication a single crystalline

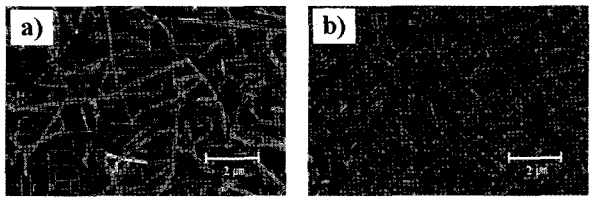

Fig. 7. Surface SEM images of YBCO films deposited on ZnO nanorods/$SrTiO_3$ for (a) 15 min and (b) 30 min.

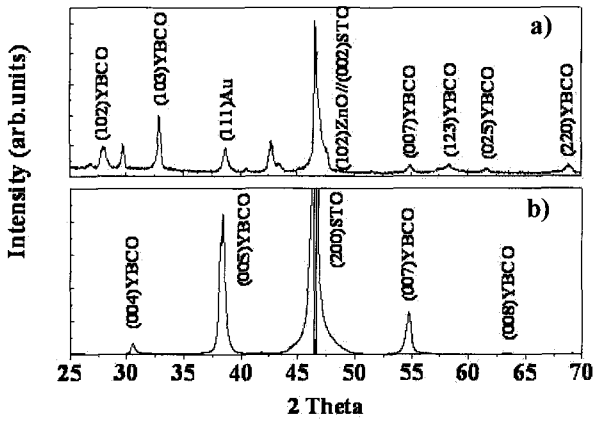

Fig. 8. X-ray diffraction patterns for (a) YBCO grown on STO with ZnO nanorods and (b) pure YBCO grown on STO.

wurtzite structure, reveal that the nanorod grow along the c-axis. Inset figure shows the selected area electron diffraction (SAED) pattern of which clearly reveals its single-crystal nature and (002) growth direction.

Photoluminescence (PL) spectra of the pure ZnO nanorod are shown in Figure 6. As illustrated in Fig. 6, a sharp strong peak that is originated from the near band-edge emission of the pure ZnO nanorods can be observed at approximately 370 nm. PL check of pure ZnO nanorod is shown in Figure 6, in which dominant peak of the exciton bound to neutral donor (D^0X) is found at 3.360 eV.

Figure 7 shows surface SEM images of YBCO films deposited on STO substrates with ZnO nanorods for 15 and 30 min, respectively. YBCO was adhered on ZnO nanorods and deposited on surface of the substrate as linear in (a). However the surface roughness became rough and many holes were also observed with increasing the deposition time from 15 to 30 min (b).

Figure 8 shows X-ray diffraction patterns of pure YBCO and YBCO grown on STO with ZnO nanorods. YBCO film deposited directly on STO substrate shows the c-axis orientation while YBCO films with ZnO nanorods exhibit mixed phases without any typical crystal orientation, related with Au (111) and ZnO (102). This suggested that the irregularly grown YBCO films were caused by growth of ZnO film and randomly aligned ZnO nanorods.

The temperature dependence of resistance for the prepared pure YBCO and YBCO deposited on STO with ZnO nanorods is shown in Figure 9. Tc was might possibly suppressed by added ZnO nanorods for flux pinning. The

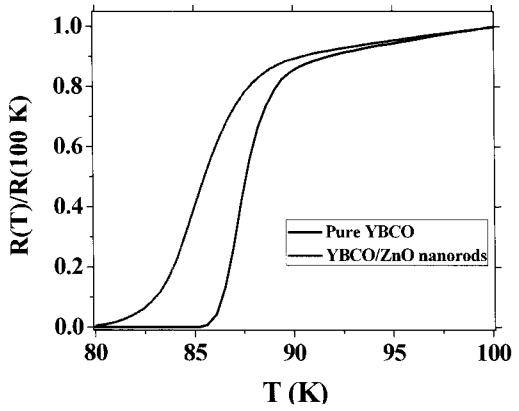

Fig. 9. Temperature dependence of normalized resistance for the pure YBCO and YBCO deposited on STO with ZnO nanorods.

fabrication of YBCO coated conductors with ZnO nanorods added to improve the pinning properties is underway, and the superconducting properties will be investigated.

4. CONCLUSIONS

To control density of ZnO nanorods, Au nanoparticles as catalyst were synthesized on STO substrates chemically modified by the formation of a self-assembled monolayer. The density of Au nanoparticles is approximately 240~260 μm^{-2} with diameters of 41~49 nm. ZnO nanorods have been grown on the substrate surface using hot-walled pulsed laser deposition. Typical size of ZnO nanorod was around 179 nm in diameter and 2~6 μm in length respectively. The ZnO nanorods have apparently randomly aligned and showed single-crystal nature along (0002) growth direction. Our preliminary results indicate that YBCO film deposited directly on STO substrate shows the c-axis orientation while YBCO films with ZnO nanorods exhibit peaks related to phases of Au (111), ZnO (102) and any mixed phases without any typical crystal orientation.

ACKNOWLEDGMENT

This work was supported by a grant from the Center for Applied Superconductivity Technology of the 21st Century Frontier R&D Program, funded by the Ministry of Education, Science and Technology, Republic of Korea.

REFERENCES

[1] D. Larbalestier, A. Gurevich, D.M. Feldmann, A. Polyanskii, "High-T_c superconducting materials for electric power applications", *Nature* 414, pp. 368, 2001.

[2] T. Haugan, P. N. Barnes, R. Wheeler, F. MeisenKothen, M. Sumption, "Additional of nanoparticle dispersions to enhance flux pinning of the $YBa_2Cu_3O_{7-x}$ superconductor", *Nature* 430, pp. 867, 2004.

[3] K. Matsumoto, T. Horide, A. Ichinose, S. Horii, Y. Yoshida, M. Mukaida, "Critical current control in $YBa_2Cu_3O_{7-\delta}$ films using artificial pinning centers", *Jpn. J. Appl. Phys.* 44, pp. L246, 2005.

[4] M. Mukaida, T. Horide, R. Kita, S. Horii, A. Ichinose, Y. Yoshida, O. Miura, K. Matsumoto, K. Yamada, N. Mori, "Critical current density enhancement around a matching field in $ErBa_2Cu_3O_{7-\delta}$ films with $BaZrO_3$ nano-rods", *Jpn. J. Appl. Phys.* 44, pp. L952, 2005.

[5] C. V. Varanasi, P. N. Barnes, L. Burke, L. Brunke, I. Maartense, T. J. Haugan, E. A. Stinzianni, K. A. Dunn, P. Haldar, "Flux pinning enhancement in $YBa_2Cu_3O_{7-x}$ films with $BaZrO_3$ nanoparticles", *Supercond. Sci. Technol.* 19, pp. L37, 2006.

[6] D. W. Kim, S. Shin, Y. Kim, S.H. Chang, Y. J. Chang, M. Kim, H. Jeong, "Growth behavior of ZnO thin films and nanowires on $SrTiO_3$ substrates", *Solid State Commun.* 143, pp. 140, 2007.

[7] J. Turkevitch, P.C. Stevenson, J. Hillier, "A study of the nucleation and growth processes in the synthesis of colloidal gold", *Discussion of the Faraday Society* 11, PP. 55, 1951.